The Crystal Structures of $[NMe_4]_2[(PhPO_3)\{MoO(O_2)_2\}_2\{MoO(O_2)_2(H_2O)\}]$ and $[NBu^n_4]_2[W_4O_6(O_2)_6(OH)_2(H_2O)_2]$ and Their Use as Catalytic Oxidants†

William P. Griffith,* Bernardeta C. Parkin, Andrew J. P. White and David J. Williams*
Department of Chemistry, Imperial College of Science, Technology and Medicine, London SW7 2AY, UK

The new trinuclear heteropolyperoxo complexes $[NMe_4]_2[(RPO_3)\{MO(O_2)_2\}_2\{MO(O_2)_2(H_2O)\}]$ (R = Ph, M = Mo **1** or W **2**) have been isolated and the crystal structure of the molybdenum complex is reported. A series of analogous molybdenum complexes (R = Me, Et, Bu^n or Bu^t; M = Mo) have also been synthesised and characterised. The use of these compounds as catalysts for the epoxidation of alkenes, oxidation of alcohols and of tertiary amines with hydrogen peroxide as cooxidant has been studied, and complex **2** is shown to be particularly effective for such oxidations. The crystal structure of the new tetranuclear isopolyperoxo species $[NBu^n_4]_2[W_4O_6(O_2)_6(OH)_2(H_2O)_2]$ **3** is also reported and its properties as a catalyst for alkene epoxidation with hydrogen peroxide as cooxidant studied.

The study of the specific oxidation of organic substrates catalysed by polyoxo[2] or polyperoxo complexes[1,3-5] is of current interest, especially because of the widespread use of the environmentally acceptable hydrogen peroxide as cooxidant in such systems. In earlier papers of this series[1,3] we have shown that analogues of 'Venturello's compound', $[N(C_6H_{13})_4]_3[PO_4\{WO(O_2)_2\}_4]$,[6] such as the arsenic species $[N(C_6H_{13})_4]_3[AsO_4\{WO(O_2)_2\}_4]$, are effective catalysts for alkene epoxidation or alcohol oxidation with H_2O_2 as cooxidant in a biphasic benzene–water mixture.[3] Recently we have shown that both of these complexes as well as the dimeric isopolyperoxo species $[W_2O_3(O_2)_4]^{2-}$ are, with hydrogen peroxide as cooxidant, good catalysts for the oxidation of tertiary amines to the corresponding *N*-oxides.[1]

Here we report the isolation and characterisation of the novel trinuclear species $[NMe_4]_2[(PhPO_3)\{MoO(O_2)_2\}_2\{MoO(O_2)_2(H_2O)\}]$ **1** and show that its tungsten analogue (**2**) is an effective oxidation catalyst for alkenes, alcohols and tertiary amines. In support of our earlier hypothesis that the presence of an asymmetrically bound η^2,η^1-peroxo moiety is desirable for effective oxidation catalysis,[3] we report the isolation and structural characterisation of a new and unusual tetranuclear isopolyperoxo species $[NBu^n_4]_2[W_4O_6(O_2)_6(OH)_2(H_2O)_2]$ **3**; this, unlike complex **1** contains only symmetric η^2-peroxo units and seems in consequence to be a less effective oxidation catalyst. The X-ray crystal structures of complexes **1** and **3** are presented and discussed; although **1** is a poor epoxidant of alkenes, **2** and **3** act as catalysts for alkene epoxidation and alcohol oxidation.

Results and Discussion

Heteropolyperoxo Trinuclear Species.—(i) *Preparation of* $[NMe_4]_2[(RPO_3)\{MoO(O_2)_2\}_2\{MoO(O_2)_2(H_2O)\}]$. These complexes were isolated as yellow crystalline solids by reacting stoichiometric quantities of $MoO_3{\cdot}H_2O$, H_2O_2, $RPO(OH)_2$ (R = Me, Et, Bu^n or Bu^t) and NMe_4Cl in water–ethanol (70:30), followed by cooling at 0 °C for 3 d.

(ii) *Preparation and crystal structure of complex* **1**. Yellow crystals of complex **1** suitable for X-ray analysis were obtained as described above. The crystal structure, Fig. 1, shows each of the three molybdenum(VI) centres to have distorted pentagonal-bipyramidal geometries. Four of the equatorial sites around each of the metal centres are occupied by two bidentate peroxo groups. The fifth site in each case is filled by a phosphonate oxygen atom [Mo–O(P) 2.014(4)–2.035(4) Å]. Selected bond lengths and angles are listed in Table 1, atomic coordinates in Table 2.

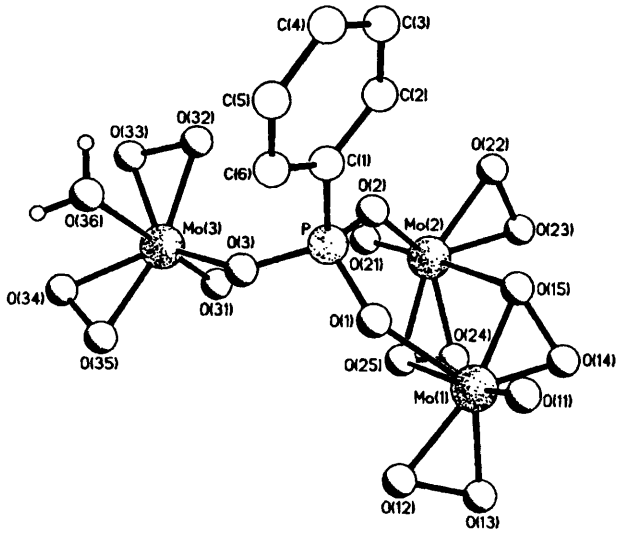

Fig. 1 Crystal structure of $[NMe_4]_2[(PhPO_3)\{MoO(O_2)_2\}_2\{MoO(O_2)_2(H_2O)\}]$ **1**

Whereas four of the six peroxo groups are of the non-bridging η^2 type [Mo–η^2(O_2) 1.906(4)–1.934(4), η^2(O–O) 1.453(6)–1.477(6) Å; O–Mo–O 44.4(2)–45.2(2)°], two of them are involved in bridging between Mo(1) and Mo(2) in an η^2,η^1 fashion. The consequence of this 'extra' interaction is not a lengthening of either peroxide bond (which remain at *ca.* 1.47 Å with an angle subtended at molybdenum of around 44.2°) but an increase in the bond length to the parent molybdenum atoms of the bridging oxygen atoms O(15) and O(25) [Mo(1)–O(14) 1.920(4), Mo(1)–O(15) 1.979(3), Mo(2)–O(24) 1.916(4) and Mo(2)–O(25) 1.985(3) Å]. The bridging bond lengths to the second metal atoms [O(15)–Mo(2) 2.478(4) and O(25)–Mo(1)

† Studies on Polyoxo- and Polyperoxo-metalates. Part 3.[1]

Supplementary data available: see Instructions for Authors, *J. Chem. Soc., Dalton Trans.*, 1995, Issue 1, pp. xxv–xxx.

Table 1 Selected bond lengths (Å) and angles (°) for complex **1** with estimated standard deviations (e.s.d.s) in parentheses

P–O(1)	1.523(4)	Mo(2)–O(22)	1.934(4)	P–O(2)	1.532(4)	Mo(2)–O(23)	1.913(4)
P–O(3)	1.509(4)	Mo(2)–O(24)	1.916(4)	P–C(1)	1.767(5)	Mo(2)–O(25)	1.985(3)
O(1)–Mo(1)	2.019(4)	O(22)–O(23)	1.477(6)	Mo(1)–O(11)	1.658(4)	O(24)–O(25)	1.471(5)
Mo(1)–O(12)	1.921(4)	O(3)–Mo(3)	2.035(4)	Mo(1)–O(13)	1.906(4)	Mo(3)–O(31)	1.658(5)
Mo(1)–O(14)	1.920(4)	Mo(3)–O(32)	1.924(5)	Mo(1)–O(15)	1.979(3)	Mo(3)–O(33)	1.911(6)
Mo(1)–O(25)	2.469(4)	Mo(3)–O(34)	1.915(4)	O(12)–O(13)	1.468(6)	Mo(3)–O(35)	1.928(4)
O(14)–O(15)	1.463(6)	Mo(3)–O(36)	2.349(6)	O(15)–Mo(2)	2.478(4)	O(32)–O(33)	1.471(8)
O(2)–Mo(2)	2.014(4)	O(34)–O(35)	1.453(6)	Mo(2)–O(21)	1.671(4)		
O(1)–P–O(2)	111.3(2)	O(22)–Mo(2)–O(23)	45.2(2)	O(1)–P–O(3)	107.9(2)	O(15)–Mo(2)–O(24)	80.8(1)
O(2)–P–O(3)	113.2(2)	O(2)–Mo(2)–O(24)	131.3(2)	O(1)–P–C(1)	108.5(2)	O(21)–Mo(2)–O(24)	101.5(2)
O(2)–P–C(1)	106.5(2)	O(22)–Mo(2)–O(24)	129.9(2)	O(3)–P–C(1)	109.4(2)	O(23)–Mo(2)–O(24)	87.4(2)
P–O(1)–Mo(1)	138.6(2)	O(15)–Mo(2)–O(25)	71.2(1)	O(1)–Mo(1)–O(11)	95.8(2)	O(2)–Mo(2)–O(25)	87.6(2)
O(1)–Mo(1)–O(12)	86.2(2)	O(21)–Mo(2)–O(25)	104.7(2)	O(11)–Mo(1)–O(12)	105.4(2)	O(22)–Mo(2)–O(25)	150.8(2)
O(1)–Mo(1)–O(13)	130.5(2)	O(23)–Mo(2)–O(25)	127.5(2)	O(11)–Mo(1)–O(13)	104.4(2)	O(24)–Mo(2)–O(25)	44.3(2)
O(12)–Mo(1)–O(13)	45.1(2)	Mo(2)–O(22)–O(23)	66.7(2)	O(1)–Mo(1)–O(14)	131.3(2)	Mo(2)–O(23)–O(22)	68.2(2)
O(11)–Mo(1)–O(14)	101.5(2)	Mo(2)–O(24)–O(25)	70.4(2)	O(12)–Mo(1)–O(14)	130.6(2)	Mo(1)–O(25)–Mo(2)	108.0(1)
O(13)–Mo(1)–O(14)	88.5(2)	Mo(1)–O(25)–O(24)	110.5(2)	O(1)–Mo(1)–O(15)	87.6(2)	Mo(2)–O(25)–O(24)	65.4(2)
O(11)–Mo(1)–O(15)	104.4(2)	P–O(3)–Mo(3)	138.8(2)	O(12)–Mo(1)–O(15)	150.0(2)	O(3)–Mo(3)–O(31)	94.3(2)
O(13)–Mo(1)–O(15)	128.3(2)	O(3)–Mo(3)–O(32)	88.1(2)	O(14)–Mo(1)–O(15)	44.0(2)	O(31)–Mo(3)–O(32)	102.9(3)
O(1)–Mo(1)–O(25)	75.6(1)	O(3)–Mo(3)–O(33)	132.7(2)	O(11)–Mo(1)–O(25)	170.4(2)	O(31)–Mo(3)–O(33)	101.9(3)
O(12)–Mo(1)–O(25)	78.6(1)	O(32)–Mo(3)–O(33)	45.1(3)	O(13)–Mo(1)–O(25)	84.7(2)	O(3)–Mo(3)–O(34)	131.2(2)
O(14)–Mo(1)–O(25)	81.7(1)	O(31)–Mo(3)–O(34)	102.1(2)	O(15)–Mo(1)–O(25)	71.5(1)	O(32)–Mo(3)–O(34)	130.8(2)
Mo(1)–O(12)–O(13)	66.9(2)	O(33)–Mo(3)–O(34)	88.5(2)	Mo(1)–O(13)–O(12)	68.0(2)	O(3)–Mo(3)–O(35)	87.5(2)
Mo(1)–O(14)–O(15)	70.1(2)	O(31)–Mo(3)–O(35)	101.6(2)	Mo(1)–O(15)–O(14)	65.8(2)	O(32)–Mo(3)–O(35)	155.4(2)
Mo(1)–O(15)–Mo(2)	107.9(1)	O(33)–Mo(3)–O(35)	130.8(2)	O(14)–O(15)–Mo(2)	111.3(3)	O(34)–Mo(3)–O(35)	44.4(2)
P–O(2)–Mo(2)	134.1(2)	O(3)–Mo(3)–O(36)	78.8(2)	O(15)–Mo(2)–O(2)	75.3(1)	O(31)–Mo(3)–O(36)	173.0(2)
O(15)–Mo(2)–O(21)	171.6(2)	O(32)–Mo(3)–O(36)	78.3(2)	O(2)–Mo(2)–O(21)	97.4(2)	O(33)–Mo(3)–O(36)	83.9(2)
O(15)–Mo(2)–O(22)	79.6(1)	O(34)–Mo(3)–O(36)	82.0(2)	O(2)–Mo(2)–O(22)	86.6(2)	O(35)–Mo(3)–O(36)	77.1(2)
O(21)–Mo(2)–O(22)	104.5(2)	Mo(3)–O(32)–O(33)	67.0(3)	O(15)–Mo(2)–O(23)	84.1(1)	Mo(3)–O(33)–O(32)	67.9(3)
O(2)–Mo(2)–O(23)	130.5(2)	Mo(3)–O(34)–O(35)	68.3(2)	O(21)–Mo(2)–O(23)	104.0(2)	Mo(3)–O(35)–O(34)	67.3(2)

Table 2 Atomic coordinates ($\times 10^4$) for complex **1**

Atom	*x*	*y*	*z*	Atom	*x*	*y*	*z*
P	−1062(1)	5978(1)	3201(1)	O(34)	−3121(5)	4018(2)	1288(3)
O(1)	267(4)	5748(2)	3646(2)	O(35)	−2151(5)	3927(2)	1949(3)
Mo(1)	2262(1)	6071(1)	3716(1)	O(36)	−4239(5)	4624(3)	2632(3)
O(11)	2399(5)	6126(3)	4675(2)	C(1)	−2259(5)	6278(3)	3873(3)
O(12)	2665(4)	5004(2)	3474(2)	C(2)	−2565(7)	7053(3)	3963(4)
O(13)	3865(4)	5518(3)	3448(3)	C(3)	−3492(8)	7278(4)	4511(4)
O(14)	3143(4)	7020(2)	3426(2)	C(4)	−4062(7)	6729(5)	4970(4)
O(15)	1651(4)	7123(2)	3378(2)	C(5)	−3733(7)	5965(4)	4890(4)
O(2)	−842(4)	6677(2)	2671(2)	C(6)	−2851(6)	5725(3)	4356(3)
Mo(2)	703(1)	7023(1)	2023(1)	N(1)	2270(5)	4281(2)	934(2)
O(21)	−74(5)	6848(2)	1155(2)	C(10)	3610(8)	3952(4)	729(6)
O(22)	178(4)	8079(2)	2265(3)	C(11)	2182(10)	4227(5)	1783(4)
O(23)	1520(4)	8028(2)	1910(2)	C(12)	1138(9)	3821(4)	555(5)
O(24)	2488(4)	6588(2)	1896(2)	C(13)	2166(8)	5105(3)	688(4)
O(25)	1647(4)	6031(2)	2312(2)	N(2)	−4567(5)	7954(2)	1337(3)
O(3)	−1606(4)	5268(2)	2770(2)	C(20)	−3051(7)	7860(4)	1318(4)
Mo(3)	−2620(1)	5002(1)	1745(1)	C(21)	−4962(7)	7719(4)	2125(4)
O(31)	−1344(5)	5282(3)	1212(3)	C(22)	−4953(9)	8784(4)	1198(5)
O(32)	−3664(6)	5945(3)	1845(4)	C(23)	−5290(8)	7452(4)	749(4)
O(33)	−4176(6)	5454(3)	1195(4)				

2.469(4) Å] are comparable with those found in $[N(C_6H_{13})_4]_3[PO_4\{WO(O_2)_2\}_4]$[6] and in $[NBu^n_4]_2[\{PO_3(OH)\}\{WO(O_2)_2\}_2]$.[7]

All three metal centres possess an axial oxo group [Mo–O_{oxo} 1.658(5)–1.671(4) Å]. For Mo(1) and Mo(2) the *trans* axial position is occupied by a bridging oxygen atom from an η^2,η^1 interaction [O(25) and O(15) respectively, see above]. The Mo(3) centre has a particularly weakly bound water molecule in this site [Mo(3)–O(36) 2.349(6) Å, *cf.* an average of 2.20 Å for terminal Mo–OH_2 groups[8]], although distances more comparable with that seen here have been observed in the isopolyperoxo species $K_2[Mo_2O_3(O_2)_4(H_2O)_2]$ (2.45 Å)[9] and $[C_5H_5NH]_2[Mo_2O_3(O_2)_4(H_2O)_2]$ [2.455(7) Å].[10]

The angles between the peroxo groups are in the range 128–130° whilst those between the bridging phosphonate donor atoms and peroxo groups are in the range 108–113° (considering each peroxo group as a unidentate ligand associated with a trigonal-bipyramidal geometry around each metal centre). In all three cases, the molybdenum centre is displaced towards the oxo group relative to the plane of the five oxygen atoms normal to this direction; the deviations are 0.41, 0.41 and 0.34 Å for Mo(1), Mo(2) and Mo(3) respectively. [The five equatorial co-ordinated oxygen atoms are coplanar to within 0.12, 0.10 and 0.07 Å for Mo(1), Mo(2) and Mo(3) respectively.] The angles between the oxo groups and the *trans* ligands are in the range 170–173°.

The geometry around the phosphorus atom is tetrahedral, with angles from 107 to 113°. The phosphorus–oxygen bond lengths do not differ significantly [P–O 1.509(4)–1.532(4) Å]. Symmetry related and lattice translated molecules are linked *via*

O–H · · · O hydrogen bonds (2.81 and 2.84 Å) between the aqua ligand in one molecule and peroxo oxygen atoms in adjacent molecules producing sheets that extend in the crystallographic *a* and *b* directions (Fig. 2).

(ii) *Vibrational and* ^{31}P-$\{^1H\}$ *NMR spectroscopy*. The infrared and Raman spectra (Table 3) of $[NMe_4]_2[(RPO_3)\{MO(O_2)_2\}_2\{MO(O_2)_2(H_2O)\}]$ (M = Mo or W; R = Ph, Me, Et, Bu^n or Bu^t) show features comparable with those observed for $[XO_4\{MO(O_2)_2\}_4]^{3-}$ and $[XO_4\{MO(O_2)_2\}_2\{MO(O_2)_2(H_2O)\}]^{3-}$ [M = Mo or W, X = P or As].[3] Bands near 970 cm^{-1} were assigned as ν(M=O), those near 870 cm^{-1} as ν(O–O) of the η^2-peroxo ligands and those around 580 and 520 cm^{-1} as asymmetric and symmetric $M(O_2)$ stretches respectively. In addition to bands due to NMe_4^+ and the phosphonic acid R group, P=O stretches appear near 1080 cm^{-1}.

The ^{31}P-$\{^1H\}$ NMR spectra of $[NMe_4]_2[(RPO_3)\{MoO(O_2)_2\}_2\{MoO(O_2)_2(H_2O)\}]$ in non-aqueous solvents show a single resonance [δ 25.30 (CD_3OD), R = Ph; δ 38.14 (CD_3OD), R = Me; δ 38.56 (CD_3OD), R = Et; δ 39.99 (CD_3OD), R = Bu^n; δ 39.42 (CD_3OD), R = Bu^t], suggesting that a single species is present in solution. Similarly, a solution of $[NMe_4]_2[(PhPO_3)\{WO(O_2)_2\}_2\{WO(O_2)_2(H_2O)\}]$ gives a 1:6:1 'triplet' at δ = 15.81 (CD_3CN) with poorly resolved tungsten satellites ($^2J_{P-W}$ = 18 Hz). As with $[PO_4\{WO(O_2)_2\}_4]^{3-}$, aqueous solutions of each of these trinuclear complexes give rise to several signals, most probably due to di- and mono-nuclear species, $[\{RP(OH)O_2\}\{MO(O_2)_2\}_2]^-$ and $[\{RP(OH)O_2\}\{MO(O_2)_2(H_2O)\}]^-$ respectively.

(iii) *Oxidations*. In the presence of the phase-transfer cation $N(C_6H_{13})_4Cl$ in a 2:1 (cation:complex) ratio, complex **2** cleanly catalyses the epoxidation of a number of cyclic and linear alkenes in biphasic 15% H_2O_2–benzene (Table 4). The epoxidation of small ring cycloalkenes are found to be more efficient than those catalysed by $[N(C_6H_{13})_4]_3[PO_4\{WO(O_2)_2\}_4]$, but the latter is the better epoxidant for larger rings.[3] Similarly (under identical reaction conditions) **2** also catalyses the oxidation of primary and secondary alcohols, although less efficiently than $[N(C_6H_{13})_4]_3[PO_4\{WO(O_2)_2\}_4]$ (Table 5).[3] Tertiary amines (*e.g.* nicotinic acid) are oxidised to the corresponding *N*-oxides in yields of 60–80%.

The molybdenum analogue, **1**, in the presence of a stoichiometric amount of $N(C_6H_{13})_4Cl$, will also catalyse alkene epoxidation, though far less efficiently than **2**. This often appears to be the case with oxidations with molybdenum and tungsten complexes in which H_2O_2 is the cooxidant.[11]

Isopolyperoxo Tetranuclear Species.—(i) *Preparation and crystal structure of complex* **3**. Colourless crystals of complex **3** were obtained by reacting stoichiometric amounts of $WO_3 \cdot H_2O$, H_2O_2 and NBu^n_4Cl in water–ethanol (70:30) acidified to pH 1.5 with H_2SO_4, followed by cooling at 0 °C for 3 d. The structural analysis of **3** reveals a complex structure containing four tungsten centres arranged around a crystallographic centre of symmetry (Fig. 3). Selected bond lengths and angles are listed in Table 6, atomic coordinates in Table 7.

Each crystallographically independent tungsten(VI) atom has a distorted pentagonal-bipyramidal geometry. One tungsten, W(1), is bound to two equatorial η^2-peroxo ligands [W(1)–$\eta^2(O_2)$ 1.878(12)–1.958(12), η^2(O–O) 1.439(18) and 1.497(15) Å, O–W–O 43.8(6) and 45.9(5)°] with the fifth equatorial position being occupied by a bridging [to W(2′)] hydroxide, O(6) [W(1)–O(6) 2.075(8) Å]. The angles between the equatorial bridging hydroxide oxygen O(6) and the two peroxo ligands are 108 and 112° with an angle of 131° between the two peroxo ligands. One of the axial sites of this metal centre is filled by an oxo ligand, O(1) [W(1)–O(1) 1.697(14) Å], whilst the other contains a triply bridging [to W(2) and W(2′)] oxide atom, O(7) [W(1)–O(7) 2.155(7) Å, O(1)–W(1)–O(7) 160.7(5)°]. The non-linearity of the axial substituents is probably due to the constraints imposed upon O(7) to permit it to be triply bridging.

The second tungsten centre, W(2), is linked equatorially to its centrosymmetric counterpart, W(2′), by a pair of μ_3-oxide atoms, O(7) and O(7′) [W(2)–O(7) 1.973(7) and W(2)–O(7′) 2.024(8) Å]. Two of the other equatorial sites are filled by an η^2-peroxo ligand [W(2)–O(8) 1.930(10), W(2)–O(9) 1.923(9), η^2(O–O) 1.522(13) Å, O–W–O 46.5(4)°] with the final position occupied by the bridging [to W(1′)] hydroxide O(6) [W(2)–O(6′) 2.038(8) Å]. Oxo, O(10), and aqua, O(11), ligands fill the axial positions [W(2)–O(10) 1.744(9), W(2)–O(11) 2.349(10) Å, O(10)–W(2)–O(11) 176.6(4)°].

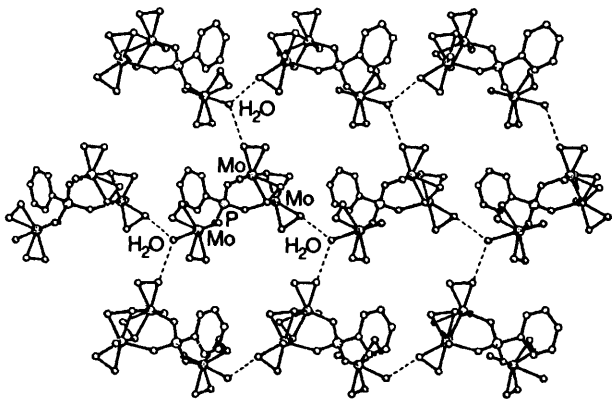

Fig. 2 Structure of complex **1** showing the intermolecular hydrogen bonding

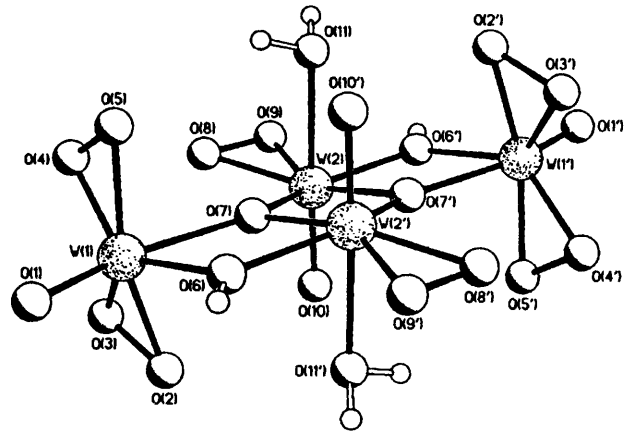

Fig. 3 Crystal structure of $[NBu^n_4]_2[W_4O_6(O_2)_6(OH)_2(H_2O)_2]$ **3**

The transannular W(2) · · · W(2′) and O(7) · · · O(7′) distances are 3.20 and 2.39 Å respectively, whilst those between W(1) and W(2′) and between O(6) and O(7) are 3.38 and 2.39 Å respectively. The tungsten atoms [W(1) and W(2)], the bridging oxygen ligands between them [O(6) and O(7)] and their centrosymmetrically related counterparts are coplanar to within 0.09 Å. In each case, the tungsten(VI) atoms are displaced towards their associated oxo groups relative to the plane of the five oxygen atoms normal to these directions; the deviations are 0.32 and 0.30 Å for W(1) and W(2) respectively. [The five equatorial co-ordinated oxygen atoms are coplanar to within 0.01 and 0.08 Å for W(1) and W(2) respectively.]

Although the positions of the hydroxy and aqua hydrogen atoms could not be definitively assigned from ΔF maps, their presence has been inferred on the basis of the tungsten–oxygen bond lengths, and their positions from their potential intermolecular hydrogen-bonding interactions. The shortness of the W(1)–O(1) and W(2)–O(10) distances (see above) clearly identifies O(1) and O(10) as oxo ligands. Similarly, the observed long W(2)–O(11) distance is diagnostic of a terminal tungsten–aqua bond. The value observed here, 2.349(10) Å, is significantly longer than the average, 2.12 Å, reported for terminal W–OH_2 ligands *trans* to oxo,[8] though very similar to that observed in

Table 3 Vibrational spectroscopic characteristics (cm^{-1})* of $[NMe_4]_2[(RPO_3)\{MO(O_2)_2\}_2\{MO(O_2)_2(H_2O)\}]$ and $[NBu^n_4]_2[W_4O_6(O_2)_6(OH)_2(H_2O)_2]$

							Other bands	
Complex	ν(M=O)	ν(O–O)	$\nu_{asym}[(M_2O)]$	$\nu_{sym}[M(O)_2]$	$\nu_{asym}[M(O)_2]$	$\nu[M(OH_2)]$	ν(OH)	δ(HOH)
1 $[NMe_4]_2[(PhPO_3)\{MoO(O_2)_2\}_2\{MoO(O_2)_2(H_2O)\}]$	964vs	869vs	768s	657s	584s	319m	3381vs	1657s
	983 (10)	*889 (9)*	*767 (2)*	—	*539 (5)*	*322 (4)*	—	—
2 $[NMe_4]_2[(PhPO_3)\{WO(O_2)_2\}_2\{WO(O_2)_2(H_2O)\}]$	956vs	847vs	768s	623s	549s	316m	3424vs	1637s
	953 (10)	*862 (3)*	*761 (2)*	*628 (1)*	*561 (4)*	*322 (5)*	—	—
$[NMe_4]_2[(MePO_3)\{MoO(O_2)_2\}_2\{MoO(O_2)_2(H_2O)\}]$	962vs	865vs	764s	648s	566s	321m	3370vs	1648s
	983 (10)	*883 (8), 878 (7)*	*752 (2)*	*657 (1)*	*560 (4)*	*325 (5)*	—	—
$[NMe_4]_2[(EtPO_3)\{MoO(O_2)_2\}_2\{MoO(O_2)_2(H_2O)\}]$	961vs	868vs	765s	651s	579s	322m	3372vs	1652s
	979 (10)	*875 (8)*	*754 (3)*	*655 (1)*	*562 (4)*	*324 (5)*	—	—
$[NMe_4]_2[(Bu^nPO_3)\{MoO(O_2)_2\}_2\{MoO(O_2)_2(H_2O)\}]$	963vs	864vs	767s	653s	580s	321m	3374vs	1655s
	980 (10)	*877 (7)*	*755 (3)*	*655 (1)*	*564 (5)*	*323 (5)*	—	—
$[NMe_4]_2[(Bu^tPO_3)\{MoO(O_2)_2\}_2\{MoO(O_2)_2(H_2O)\}]$	963vs	863vs	764s	652s	581s	320m	3376vs	1653s
	982 (10)	*875 (8)*	*754 (2)*	*656 (1)*	*561 (4)*	*323 (5)*	—	—
3 $[NBu^n_4]_2[W_4O_6(O_2)_6(OH)_2(H_2O)_2]$	969vs, 943vs	874vs, 854vs	748s	657s	583vs, 570vs	—	3338vs	1637s
	967 (10), 959 (9)	*858 (4)*	—	*638 (1)*	*567 (8)*	*312 (6)*	—	—

* Raman data in italics (relative intensities in parentheses).

$K_2[W_2O_3(O_2)_4(H_2O)_2]\cdot 2H_2O$,[12] emphasising the weak nature of the binding of the aqua ligand in these species. The proximity in the crystal of O(6) and of O(1) of a lattice-translated complex [2.57(2) Å] is too short for a non-hydrogen-bonded O···O approach, thus O(6) must be protonated. Consideration of charges and formal oxidation states rules out the possibility of a bridging aqua ligand.

The role of the aforementioned hydrogen-bonding interaction is significant in determining the packing of the complexes in the crystal. Lattice-translated molecules are linked by pairs of O–H···O hydrogen bonds between O(1) and O(6′) and between O(1′) and O(6) across a crystallographic symmetry centre producing a hydrogen-bonded chain of molecules that extends in the crystallographic *a* direction (Fig. 4). The partial-occupancy hydrate molecule is positioned such as to be able to form intra-complex hydrogen bonds *via* one long and two short interactions [O(50)···O(5) 2.35(3), O(50)···O(11) 2.45(4) and O(50)···O(10′) 2.90(4) Å]. Due to the symmetry within the complex, there are two of these 50%-occupancy water molecules per tetratungsten anion.

The structure of complex **3** reported here has gross features very similar to those observed in the analogous molybdenum complex $[NBu^n_4]_2[Mo_4O_6(O_2)_6(HOMe)_2(OMe)_2]$.[13] In this latter species two of the axial and two of the Mo···X···Mo bridging positions have been replaced by OMe and MeOH groups respectively. The authors did not, however, indicate how a differentiation between the identities of these two substituents was achieved.

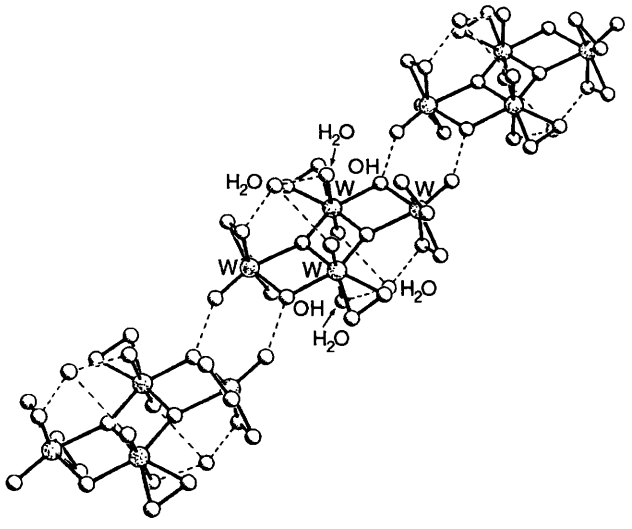

Fig. 4 Structure of complex **3** showing the intermolecular hydrogen bonding

(ii) *Oxidations*. Epoxidation of cyclic and linear alkenes by $[N(C_6H_{13})_4]_2[W_4O_6(O_2)_6(OH)_2(H_2O)_2]$ [generated by addition of two equivalents of $N(C_6H_{13})_4Cl$ to complex **3**] in biphasic 15% H_2O_2–benzene gave epoxides in much poorer yields than those observed for $[N(C_6H_{13})_4]_3[XO_4\{WO(O_2)_2\}_4]$ (X = P or As)[3] or $[N(C_6H_{13})_4]_2[W_2O_3(O_2)_4]$[1] (Table 4). Although the reasons for the poor catalytic activity of **3** are not immediately apparent, we believe that the absence of η^2,η^1-peroxide linkages are a determining factor.

Conclusion

It is clear that complex **3**, which contains six conventional symmetric η^2-peroxo groups and none of the asymmetric η^2,η^1-counterparts is a far less effective alkene epoxidant than complex **2** (under similar reaction conditions). Although we were unable to obtain crystals of **2** to allow a direct comparison of its structure with that of **1**, it is thought likely that they have similar structures.

In general, it seems that tungsten complexes containing asymmetric η^2,η^1-peroxo ligands are efficient epoxidation catalysts with H_2O_2 as cooxidant, *cf.* $[N(C_6H_{13})_4]_3[PO_4\{WO(O_2)_2\}_4]$[6] and $[NBu^n_4]_2[\{PO_3(OH)\}\{WO(O_2)_2\}_2]$.[7] The compounds $Q_2[W_2O_3(O_2)_4]$ [Q = PPh_4, $AsPh_4$, Ph_3PCH_2Ph or $N(C_6H_{13})_4$] are also believed to contain asymmetric peroxo units,[1] and have been shown to be active epoxidation

Table 4 Oxidation of linear and cyclo alkenes by $[(PhPO_3)\{WO(O_2)_2\}_2\{WO(O_2)_2(H_2O)\}]^{2-}$ and $[W_4O_6(O_2)_6(OH)_2(H_2O)_2]^{2-}$

		Yield (%) [Turnover]	
Substrate	Product	**2**	**3**
Cyclopentene	1,2-Epoxycyclopentane	87 [168]	4 [8]
Cyclohexene	1,2-Epoxycyclohexane	22 [43]	2 [4]
Cycloheptene	1,2-Epoxycycloheptane	73 [141]	—
Cyclooctene	1,2-Epoxycyclooctane	95 [183]	21 [41]
Cyclododecene	1,2-Epoxycyclododecane	67 [129]	6 [12]
cis-Stilbene	*cis*-2,3-Diphenyloxirane	59 [114]	—
trans-Stilbene	*trans*-2,3-Diphenyloxirane	78 [151]	—
Hex-1-ene	1,2-Epoxyhexane	34 [66]	1 [2]
Hept-1-ene	1,2-Epoxyheptane	57 [110]	—
Oct-1-ene	1,2-Epoxyoctane	53 [103]	5 [10]
Non-1-ene	1,2-Epoxynonane	48 [93]	—
Dec-1-ene	1,2-Epoxydecane	55 [106]	6 [12]
Undec-1-ene	1,2-Epoxyundecane	51 [99]	—
Dodec-1-ene	1,2-Epoxydodecane	48 [93]	4 [8]

Table 5 Oxidation of primary and secondary alcohols by $[(PhPO_3)\{WO(O_2)_2\}_2\{WO(O_2)_2(H_2O)\}]^{2-}$

Substrate	Product	Yield (%)	Turnover*
Benzyl alcohol	Benzaldehyde	35	71
2-Methylbenzyl alcohol	2-Methylbenzaldehyde	42	84
4-Methylbenzyl alcohol	4-Methylbenzaldehyde	28	56
4-Methoxybenzyl alcohol	4-Methoxybenzaldehyde	14	29
Piperonyl alcohol	Piperonaldehyde	34	68
(±)-Menthol	(±)-Menthone	16	33
1,2,3,4-Tetrahydronaphthol	3,4-Dihydro-2*H*-naphthalen-1-one	9	19
(±)-1-Phenylethanol	Acetophenone	91	182
2-Phenylethanol	2-Phenylethanal	31	62
Cyclopentanol	Cyclopentanone	32	64
Cyclohexanol	Cyclohexanone	33	67
2-Methylcyclohexanol	2-Methylcyclohexanone	69	137
3-Methylcyclohexanol	3-Methylcyclohexanone	90	179
4-Methylcyclohexanol	4-Methylcyclohexanone	91	183
Cycloheptanol	Cycloheptanone	52	105
Cyclooctanol	Cyclootanone	48	96

* Turnover = mol product/mol catalyst.

Table 6 Selected bond lengths (Å) and angles (°) for complex **3** with e.s.d.s in parentheses

W(1)–O(1)	1.697(14)	W(1)–O(2)	1.958(12)
W(1)–O(3)	1.878(12)	W(1)–O(4)	1.907(12)
W(1)–O(5)	1.954(13)	W(1)–O(6)	2.075(8)
W(1)–O(7)	2.155(7)	O(2)–O(3)	1.497(15)
O(4)–O(5)	1.439(18)	O(7)–W(2)	1.973(7)
W(2)–O(8)	1.930(10)	W(2)–O(9)	1.923(9)
W(2)–O(10)	1.744(9)	W(2)–O(11)	2.349(10)
W(2)–O(6′)	2.038(8)	W(2)–O(7′)	2.024(8)
O(8)–O(9)	1.522(13)		
O(1)–W(1)–O(2)	97.8(8)	O(1)–W(1)–O(3)	103.6(7)
O(2)–W(1)–O(3)	45.9(5)	O(1)–W(1)–O(4)	105.3(7)
O(2)–W(1)–O(4)	131.9(6)	O(3)–W(1)–O(4)	87.4(5)
O(1)–W(1)–O(5)	101.5(9)	O(2)–W(1)–O(5)	160.6(7)
O(3)–W(1)–O(5)	129.6(5)	O(4)–W(1)–O(5)	43.8(6)
O(1)–W(1)–O(6)	91.9(5)	O(2)–W(1)–O(6)	86.3(4)
O(3)–W(1)–O(6)	130.8(4)	O(4)–W(1)–O(6)	133.3(4)
O(5)–W(1)–O(6)	90.8(5)	O(1)–W(1)–O(7)	160.7(5)
O(2)–W(1)–O(7)	80.9(4)	O(3)–W(1)–O(7)	89.3(4)
O(4)–W(1)–O(7)	89.2(5)	O(5)–W(1)–O(7)	80.2(6)
O(6)–W(1)–O(7)	68.9(3)	W(1)–O(2)–O(3)	64.2(6)
W(1)–O(3)–O(2)	69.9(6)	W(1)–O(4)–O(5)	69.8(7)
W(1)–O(5)–O(4)	66.4(7)	W(1)–O(6)–W(2′)	110.7(4)
W(1)–O(7)–W(2)	144.9(4)	W(1)–O(7)–W(2′)	108.1(3)
W(2)–O(7)–W(2′)	106.5(3)	O(7)–W(2)–O(8)	83.2(4)
O(7)–W(2)–O(9)	129.4(4)	O(8)–W(2)–O(9)	46.5(4)
O(7)–W(2)–O(10)	95.6(4)	O(8)–W(2)–O(10)	102.7(5)
O(9)–W(2)–O(10)	99.9(4)	O(7)–W(2)–O(11)	82.9(4)
O(8)–W(2)–O(11)	80.2(4)	O(9)–W(2)–O(11)	83.4(4)
O(10)–W(2)–O(11)	176.6(4)	O(7)–W(2)–O(6′)	144.7(3)
O(8)–W(2)–O(6′)	125.2(3)	O(9)–W(2)–O(6′)	80.2(3)
O(10)–W(2)–O(6′)	97.3(4)	O(11)–W(2)–O(6′)	82.3(4)
O(7)–W(2)–O(7′)	73.5(3)	O(8)–W(2)–O(7′)	149.7(4)
O(9)–W(2)–O(7′)	148.3(3)	O(10)–W(2)–O(7′)	98.6(4)
O(11)–W(2)–O(7′)	78.0(3)	O(6′)–W(2)–O(7′)	72.2(3)
W(2)–O(8)–O(9)	66.5(5)	W(2)–O(9)–O(8)	67.0(5)

catalysts. Very recently a vanadium complex containing such ligands, $[NH_4]_5[PO_4\{VO(O_2)_2\}_2]\cdot H_2O$, has been reported.[14]

Various suggestions have been made in an effort to explain the apparent correlation between asymmetric η^2,η^1-peroxo ligation and catalytic activity in tungsten complexes.[1,3] These include ion-pairing effects,[15] facile generation of a vacant metal co-ordination site[6] and O–O bond lengthening.[16,17] We believe, as proposed by Venturello *et al.*,[6] that the most feasible explanation for the reactivity of species containing asymmetric η^2,η^1-peroxo units is that the asymmetry leads to one oxygen atom being more electrophilic than the other. This would facilitate nucleophilic attack by the alkene on the peroxide, as suggested by Sharpless *et al.*[18]

Clearly, further research into these catalysts is required before more confident hypotheses on the mechanism of the epoxidation process can be made. Of particular importance will be detailed structural information pertaining to the nature of symmetric and asymmetric peroxo ligation.

Experimental

Crystal Structure Determinations.—Crystal data for complex **1**. $C_{14}H_{31}Mo_3N_2O_{19}P$, M = 850.2, monoclinic, space group $P2_1/n$, a = 9.749(3), b = 17.154(5), c = 17.282(5) Å, β = 93.06(2)°, U = 2886(2) Å^3, Z = 4, D_c = 1.96 g cm^{-3}, μ(Mo-Kα) = 14 cm^{-1}, $F(000)$ = 1688. A yellow block of dimensions 0.73 × 0.50 × 0.40 mm was used.

Data collection and processing. Data were measured on a Siemens P4/PC diffractometer with Mo-Kα radiation (graphite monochromator) using ω scans. 5096 Independent reflections were measured ($2\theta \leqslant 50°$) of which 4364 had $|F_o| > 4\sigma(|F_o|)$ and were considered to be observed. The data were corrected for Lorentz and polarisation factors.

Structure analysis and refinement. The structure was solved by direct methods. The non-hydrogen atoms were refined anisotropically. The hydrogen atoms on the aqua ligand were located from a ΔF map and refined isotropically subject to distance and angle constraints. The positions of the remaining hydrogen atoms were idealised (C–H 0.96 Å), assigned isotropic thermal parameters, $U(H) = 1.2U_{eq}(C)$, and allowed to ride on their parent carbon atoms. Refinement, based on F, was by full-matrix least squares to give R = 0.043, R' = 0.048 [$R = \Sigma||F_o| - |F_c||/\Sigma|F_o|$, $R' = \Sigma w^{\frac{1}{2}}||F_o| - |F_c||/\Sigma w^{\frac{1}{2}}|F_o|$, $w^{-1} = \sigma^2(F) + 0.0007F^2$]. The maximum and minimum residual electron densities in the final ΔF map were 0.83 and −0.90 e Å^{-3} respectively. The mean and maximum shift/error ratios in the final refinement cycle were 0.005 and 0.021 respectively.

Crystal data for complex **3**. $C_{32}H_{78}N_2O_{22}W_4\cdot H_2O$, M = 1596.4, monoclinic, space group $P2_1/n$, a = 9.725(4), b = 18.580(11), c = 14.738(7) Å, β = 103.87(2)°, U = 2586(2) Å^3, Z = 2 (the molecule has crystallographic C_i symmetry), D_c = 2.05 g cm^{-3}, μ(Mo-Kα) = 89 cm^{-1}, $F(000)$ = 1532. A clear block of dimensions 0.27 × 0.27 × 0.30 mm was used, coated in epoxy resin to inhibit desolvation.

Data collection and processing. Data were measured on a Siemens P4/PC diffractometer with Mo-Kα radiation (graphite monochromator) using ω scans. 4560 Independent reflections were measured ($2\theta \leqslant 50°$) of which 3308 had $|F_o| > 4\sigma(|F_o|)$ and were considered to be observed. The data were corrected for Lorentz and polarisation factors and an empirical absorption correction was applied; the maximum and minimum transmission factors were 0.53 and 0.07 respectively.

Structure analysis and refinement. The structure was solved by direct methods. The full-occupancy non-hydrogen atoms were refined anisotropically. The structure was found to contain a partial-occupancy water molecule which was refined isotropically with a fixed occupancy of 0.50. The positions of the hydrogen atoms of the counter ion were idealised (C–H 0.96

Table 7 Atomic coordinates ($\times 10^4$) for complex **3**

Atom	x	y	z
W(1)	6 999(1)	868(1)	4 880(1)
O(1)	5 242(13)	914(7)	4 838(15)
O(2)	6 840(12)	673(6)	3 553(8)
O(3)	7 192(10)	1 433(6)	3 861(8)
O(4)	7 837(15)	1 644(6)	5 669(10)
O(5)	7 827(19)	1 002(7)	6 214(9)
O(6)	7 016(8)	−240(4)	5 052(7)
O(7)	9 082(7)	433(4)	4 974(5)
W(2)	10 991(1)	639(1)	4 798(1)
O(8)	10 542(9)	1 610(5)	5 092(8)
O(9)	12 057(9)	1 520(5)	4 999(7)
O(10)	10 497(10)	630(5)	3 579(6)
O(11)	11 617(11)	579(5)	6 437(7)
N	4 823(12)	2 098(7)	7 710(8)
C(10)	3 888(16)	2 399(8)	6 842(11)
C(11)	3 492(17)	3 199(9)	6 896(11)
C(12)	2 479(20)	3 437(10)	5 979(12)
C(13)	2 053(24)	4 225(11)	6 087(14)
C(20)	4 113(16)	2 101(9)	8 538(10)
C(21)	2 750(17)	1 671(10)	8 410(13)
C(22)	2 226(26)	1 706(12)	9 287(15)
C(23)	866(27)	1 387(16)	9 269(20)
C(30)	5 171(15)	1 327(8)	7 485(11)
C(31)	6 161(22)	902(9)	8 220(13)
C(32)	6 471(21)	175(9)	7 927(14)
C(33)	7 593(25)	−197(12)	8 551(18)
C(40)	6 168(14)	2 533(8)	8 039(10)
C(41)	7 092(16)	2 596(9)	7 359(12)
C(42)	8 434(16)	3 011(9)	7 780(13)
C(43)	9 409(18)	3 059(11)	7 134(13)
O(50)	9 881(35)	742(18)	7 383(26)

Å), assigned isotropic thermal parameters, $U(H) = 1.2U_{eq}(C)$, and allowed to ride on their parent carbon atoms. Refinement, based on F, was by full-matrix least squares to give $R = 0.051$, $R' = 0.050$ [$w^{-1} = \sigma^2(F) + 0.0007F^2$]. The maximum and minimum residual electron densities in the final ΔF map were 2.60 and −2.36 e Å^{-3} respectively. This high residual electron density is due to two remaining peaks of over 2.5 e less than 0.85 Å away from the two tungsten atoms (probably due to residual absorption effects). With the exception of these peaks, the residual electron density drops to 1.7 e. Many different absorption corrections including face-indexed numerical and semi-empirical based on azimuthal scans were tried, but an empirical correction using SHELXA-90[19] gave the lowest residual electron density (and R factor). The mean and maximum shift/error ratios in the final refinement cycle were 0.000 and 0.000 respectively.

For both structures, computations were carried out on a 50 MHz 486DX PC computer using the SHELXTL PC program system.[20]

Additional material available from the Cambridge Crystallographic Data Centre comprises H-atom coordinates, thermal parameters and remaining bond lengths and angles.

General.—Infrared spectra of the solids were measured over the range 4000–200 cm^{-1} using KBr discs on a Perkin-Elmer 1720 Fourier-transform spectrometer, Raman spectra of the solids (as powders in melting-point tubes) on a Perkin-Elmer 1760X FT-IR instrument fitted with a 1700X NIR FT-Raman accessory using a Nd:YAG laser (1064 nm excitation). The NMR spectra were obtained on a JEOL ESX 270 spectrometer (^{31}P, 109.25 MHz) as CD_3OD or CD_3CN solutions, using external H_3PO_4 as reference. The gas chromatography data were obtained on a Perkin-Elmer Autosystem instrument using a Perkin-Elmer stainless-steel column (2 m) packed with 5% Carbowax 20M on Chromasorb WHP AW (DCMS treated). Microanalyses were carried out by the Microanalytical Laboratories at Imperial College.

The trioxides $MoO_3{\cdot}H_2O$ and $WO_3{\cdot}H_2O$ were obtained from BDH and Fluka Chemie AG, respectively, and $PhPO(OH)_2$, $MePO(OH)_2$, $EtPO(OH)_2$, $Bu^nPO(OH)_2$, $Bu^tPO(OH)_2$, NMe_4Cl and $NBu^n{}_4Cl$ were purchased from Aldrich; each of these materials was used without further purification. Hydrogen peroxide was obtained from BDH as a 30% w/v aqueous solution and was used as supplied.

Syntheses.—$[NMe_4]_2[(PhPO_3)\{MoO(O_2)_2\}_2\{MoO(O_2)_2(H_2O)\}]$ **1**. Hydrated molybdenum trioxide, $MoO_3{\cdot}H_2O$ (1.44 g, 10.0 mmol), was suspended in aqueous hydrogen peroxide solution (7 cm^3, 30% w/v) and the resulting suspension stirred at 30 °C until a yellow solution was obtained. Upon cooling to ambient temperature, $PhPO(OH)_2$ (0.53 g, 3.33 mmol) in water (5 cm^3) was added followed by dropwise addition of NMe_4Cl (0.73 g, 6.67 mmol) in water (10 cm^3). Ethanol (5 cm^3) was added and the mixture was cooled to −15 °C. The bright yellow crystalline solid was filtered off, washed with cold ethanol (2 × 5 cm^3) and diethyl ether (10 cm^3) and air dried. Yield 2.1 g, 2.47 mmol (74%) (Found: C, 19.7; H, 3.6; N, 3.1; O_2^{2-}, 22.4. Calc. for $C_{14}H_{31}Mo_3N_2O_{19}P$: C, 19.8; H, 3.7; N, 3.3; O_2^{2-}, 22.6%). ^{31}P-{^{1}H} NMR (CD_3OD): δ 25.30.

$[NMe_4]_2[(PhPO_3)\{WO(O_2)_2\}_2\{WO(O_2)_2(H_2O)\}]{\cdot}EtOH$ **2**. Hydrated tungsten trioxide, $WO_3{\cdot}H_2O$ (2.50 g, 10.0 mmol), was suspended in aqueous hydrogen peroxide solution (7 cm^3, 30% w/v) and the resulting suspension stirred at 50 °C until a colourless solution was obtained. The solution was centrifuged to remove any undissolved residue then $PhPO(OH)_2$ (0.53 g, 3.33 mmol) in water (5 cm^3) was added followed by dropwise addition of NMe_4Cl (0.73 g, 6.67 mmol) in water (10 cm^3). Ethanol (5 cm^3) was added and the mixture was cooled to −15 °C. The colourless microcrystalline solid was filtered off, washed with cold ethanol (2 × 5 cm^3) and diethyl ether (10 cm^3) and air dried. Yield 2.8 g, 2.42 mmol (73%) (Found: C, 16.7; H, 2.8; N, 2.4; O_2^{2-}, 16.4. Calc. for $C_{16}H_{37}N_2O_{20}PW_3$: C, 16.6; H, 3.2; N, 2.4; O_2^{2-}, 16.7%). ^{31}P-{^{1}H} NMR (CD_3CN): δ 15.81 ($^2J_{P-W}$ = 18 Hz).

$[NMe_4]_2[(RPO_3)\{MoO(O_2)_2\}_2\{MoO(O_2)_2(H_2O)\}]$ (R = Me, Et, Bu^n *or* Bu^t). These complexes were prepared by a similar procedure to that described above giving yellow crystalline solids. R = Me, yield 2.2 g, 2.79 mmol (84%) (Found: C, 13.9; H, 3.4; N, 3.6; O_2^{2-}, 24.1. Calc. for $C_9H_{29}Mo_3N_2O_{19}P$: C, 13.7; H, 3.7; N, 3.6; O_2^{2-}, 24.4%). ^{31}P-{^{1}H} NMR (CD_3OD): δ 38.14. R = Et, yield 1.8 g, 2.24 mmol (67%) (Found: C, 14.9; H, 3.7; N, 3.6. Calc. for $C_{10}H_{31}Mo_3N_2O_{19}P$: C, 15.0; H, 4.0; N, 3.5%). ^{31}P-{^{1}H} NMR (CD_3OD): δ 38.56. R = Bu^n, yield 2.3 g, 2.77 mmol (83%) (Found: C, 17.4; H, 4.0; N, 3.4. Calc. for $C_{12}H_{35}Mo_3N_2O_{19}P$: C, 17.4; H, 4.3; N, 3.4%). ^{31}P-{^{1}H} NMR (CD_3OD): δ 39.99. R = Bu^t, yield 2.4 g, 2.89 mmol (87%) (Found: C, 17.5; H, 4.0; N, 3.4. Calc. for $C_{12}H_{35}Mo_3N_2O_{19}P$: C, 17.4; H, 4.3; N, 3.4%). ^{31}P-{^{1}H} NMR (CD_3OD): δ 39.42.

$[NBu^n{}_4]_2[W_4O_6(O_2)_6(OH)_2(H_2O)_2]$ **3**. Hydrated tungsten trioxide, $WO_3{\cdot}H_2O$ (1.25 g, 5.0 mmol), was suspended in hydrogen peroxide (4 cm^3, 30% w/v) and stirred at 50 °C until a colourless solution was obtained. The mixture was centrifuged to remove any insoluble residues and the resulting solution was adjusted to pH 1.5 with H_2SO_4 (2.0 mol dm^{-3}). Tetrabutylammonium chloride (2.78 g, 10.0 mmol) in water (10 cm^3) was added dropwise. Ethanol (5 cm^3) was added and the solution cooled to 4 °C. The colourless crystalline solid was filtered off, washed with cold ethanol (2 × 5 cm^3) and diethyl ether (10 cm^3) and air dried. Yield 1.25 g, 0.79 mmol (63%) (Found: C, 24.6; H, 4.8; N, 1.8; O_2^{2-}, 12.5. Calc. for $C_{32}H_{78}N_2O_{22}W_4$: C, 24.4; H, 5.0; N, 1.8; O_2^{2-}, 12.2%).

General Procedure for Expoxidation of Cycloalkenes.—The catalyst (**2** or **3**) (0.06 mmol) was dissolved in benzene (5 cm^3) and the cycloalkene (25 mmol) was added. Hydrogen peroxide (15% w/v, 6 cm^3) was added to the organic component and the biphasic mixture was refluxed at 70 °C for 3 h. The resulting organic layer was then analysed by gas chromatography.

General Procedure for Epoxidation of Linear Alkenes.—The catalyst (**2** or **3**) (0.06 mmol) was dissolved in benzene (5 cm^3) and the alkene (10 mmol) was added. Hydrogen peroxide (15% w/v, 12 cm^3) was added to the benzene solution and the biphasic mixture was refluxed at 70 °C for 20 h. The resulting organic layer was then analysed by gas chromatography and/or by ^{1}H NMR spectroscopy.

General Procedure for Oxidation of Primary and Secondary Alcohols.—The catalyst (**2**) (0.06 mmol) was dissolved in benzene (5 cm^3) and the alcohol (10 mmol) was added. Hydrogen peroxide (15% w/v, 10 cm^3) was added to the benzene solution and the biphasic mixture was refluxed at 70 °C for 3 h. The resulting organic layer was then analysed by gas chromatography and/or by gas chromatography/mass spectrometry.

Acknowledgements

We thank the EPSRC for a postdoctoral fellowship to one of us (B. C. P.), the University of London Intercollegiate Research Service for the Raman spectrometer and the EPSRC for the X-ray diffractometer.

References

1 A. J. Bailey, W. P. Griffith and B. C. Parkin, *J. Chem. Soc., Dalton Trans.*, 1995, 1833.
2 N. Mizuno and M. Misono, *J. Mol. Catal.*, 1994, **86**, 319; W. P. Griffith, *Transition Met. Chem.*, 1991, **16**, 548; M. T. Pope and A. Müller, *Angew. Chem., Int. Ed. Engl.*, 1991, **30**, 34.
3 A. C. Dengel, W. P. Griffith and B. C. Parkin, *J. Chem. Soc., Dalton Trans.*, 1993, 2683.

4 D. C. Duncan, R. C. Chambers, E. Hecht and C. L. Hill, *J. Am. Chem. Soc.*, 1995, **117**, 681; S. Sakaue, T. Tsubakino, Y. Nishiyama and Y. Ishii, *J. Org. Chem.*, 1993, **58**, 3633; Y. Ishii, H. Tanaka and Y. Nishiyama, *Chem. Lett.*, 1994, 1; C. Venturello and R. D'Aloisio, *J. Org. Chem.*, 1988, **53**, 1553; C. Venturello and M. Gambaro, *Synthesis*, 1989, **4**, 295; C. Aubry, G. Chottard, N. Platzer, J.-M. Brégeault, R. Thouvenot, F. Chauveau, C. Huet and H. Ledon, *Inorg. Chem.*, 1991, **30**, 4409.
5 D. C. Duncan, R. C. Chambers, E. Hecht and C. L. Hill, *J. Am. Chem. Soc.*, 1995, **117**, 681.
6 C. Venturello, R. D'Aloisio, J. C. J. Bart and M. Ricci, *J. Mol. Catal.*, 1985, **32**, 107.
7 L. Salles, C. Aubry, R. Thouvenot, F. Robert, C. Dorémieux-Morin, G. Chottard, H. Ledon, V. Jeannin and J.-M. Brégeault, *Inorg. Chem.*, 1994, **33**, 871.
8 A. G. Orpen, L. Brammer, F. H. Allen, O. Kennard, D. G. Watson and R. Taylor, *J. Chem. Soc., Dalton Trans.*, 1989, S1.
9 R. Stomberg, *Acta Chem. Scand.*, 1968, **22**, 1076.
10 J.-M. Le Carpentier, A. Mitschier and R. Weiss, *Acta Crystallogr., Sect. B*, 1972, **28**, 1288.
11 G. Amato, A. Arcoria, F. P. Ballistreri, G. A. Tomaselli, O. Bortolini, C. Conte, F. di Furia, G. Modena and G. Valle, *J. Mol. Catal.*, 1986, **37**, 165.
12 F. W. B. Einstein and B. R. Penfold, *Acta Crystallogr.*, 1964, **17**, 1127.
13 S. Campestrini, F. di Furia, P. Rossi, A. Torboli and G. Valle, *J. Mol. Catal.*, 1993, **83**, 95.
14 P. Schwendt, J. Tyršelová and F. Pavelčík, *Inorg. Chem.*, 1995, **34**, 1964.
15 L. J. Csányi and K. Jáky, *J. Catal.*, 1991, **127**, 42.
16 L. Salles, C. Aubry, F. Robert, G. Chottard, R. Thouvenot, H. Ledon and J.-M. Brégeault, *New J. Chem.*, 1993, **17**, 367.
17 F. P. Ballistreri, G. A. Tomaselli, R. M. Toscano, V. Conte and F. di Furia, *J. Mol. Catal.*, 1994, **89**, 293.
18 K. B. Sharpless, A. Y. Teranishi and J.-E. Backväll, *J. Am. Chem. Soc.*, 1977, **99**, 3120.
19 G. M. Sheldrick, personal communication.
20 SHELXTL PC, Release 4.1, Siemens Analytical X-Ray Instruments, Madison, WI, 1990.

Received 13*th April* 1995; *Paper* 5/02404H